Irabien, M.J.; Cearreta, A.; Gómez-Arozamena, J.; Serrano, H.; Sánchez-Cabeza, J.A. & Ruiz-Fernández, A.C. (2019). Geological record of extreme floods and anthropogenic impacts on an industrialised bay: the inner Abra of Bilbao (northern Spain). Science of the Total Environment 696: 133946.
DOI: 10.1016/j.scitotenv.2019.133946

GEOLOGICAL RECORD OF EXTREME FLOODS AND ANTHROPOGENIC IMPACTS ON AN INDUSTRIALISED BAY: THE INNER ABRA OF BILBAO (NORTHERN SPAIN)

María Jesús Irabien[1], Alejandro Cearreta[2], José Gómez-Arozamena[3], Humberto Serrano[2], Joan-Albert Sánchez-Cabeza[4], Ana Carolina Ruiz-Fernández[5]

[1]Departamento de Mineralogía y Petrología, Facultad de Ciencia y Tecnología, Universidad del País Vasco UPV/EHU, Apartado 644, 48080 Bilbao, Spain. mariajesus.irabien@ehu.eus

[2]Departamento de Estratigrafía y Paleontología, Facultad de Ciencia y Tecnología, Universidad del País Vasco UPV/EHU, Apartado 644, 48080 Bilbao, Spain. alejandro.cearreta@ehu.eus, humberto.serrano@ehu.eus

[3]Departamento de Ciencias Médicas y Quirúrgicas, Universidad de Cantabria UC, Avenida. Herrera Oria s/n, 39011 Santander, Spain. jose.gomez@unican.es

[4]Unidad Académica Procesos Oceánicos y Costeros, Instituto de Ciencias del Mar y Limnología, Universidad Nacional Autónoma de México, 04510 Ciudad de México, México. jasanchez@cmarl.uman.mx

[5]Unidad Académica Mazatlán, Instituto de Ciencias del Mar y Limnología, Universidad Nacional Autónoma de México, Calz. Joel Montes Camarena s/n, 82000 Mazatlán, Sinaloa, México. caro@ola.icmyl.unam.mx

Corresponding author: María Jesús Irabien

Highlights

- Historically contaminated estuarine sediments remain in the inner Abra of Bilbao
- Contaminated deposits are gradually covered by a layer of “cleaner” sediments
- Sediments remobilised by extreme floods can be recognised in the sedimentary record
- Both natural events and human activities can impact environmental improvement

ABSTRACT

The Bilbao estuary is one of the most polluted areas on the northern coast of Spain, owing to the direct disposal of urban effluents and wastewaters from mining and industrial activities that has occurred during the last 170 years. Recent sediment records collected from the inner Abra of Bilbao bay were examined using a multidisciplinary approach including geochemical, micropaleontological and isotopic proxies to evaluate heavy metal contamination (Pb, Zn and Cd), ecological condition (benthic foraminifera), and sediment accumulation variability (^{210}Pb). Results evidenced the interplay of both human activities and extreme weather events. Most contaminated materials are buried below a thin layer (< 25 cm) of cleaner sediments which have been deposited since contaminant discharges have substantially decreased, due to industrial reconversion and environmental regulations. However, the fingerprint left in the sedimentary record by the catastrophic floods of 1983 confirms the potential of natural events for sediment relocation, showing catastrophic events may endanger recently-achieved environmental improvements in historically contaminated coastal areas.

Keywords: Metals; Benthic foraminifera; Radionuclides; Sedimentary record; Extreme floods; Environmental improvement

1. Introduction

Estuaries are globally recognised as one of the most productive and threatened ecosystems (Robb, 2014). During the 20th century, more than 50% of coastal wetlands were lost worldwide owing to natural and anthropogenic factors such as land reclamation, aquaculture, navigation and shipping, dredging and filling operations, water extraction, decreased sediment input from catchments, sea-level rise, and

erosion (Kennish, 2002; Li et al., 2018). Although some changes may be locally reversed (Bowron et al., 2009; Cearreta et al., 2013; Mossman et al., 2012), most estuary infrastructure (artificial channels, dykes and port facilities) is usually constructed on a permanent basis, leading to the definitive transformation of original morphological and hydrodynamic features. Along with physical destruction, pollution in estuaries ranks amongst the most serious and ubiquitous problems. Land-based activities account for roughly 80% of pollutants released to the marine environment (World Wildlife Foundation, 2015) and transitional areas can act not only as a reservoir for a long list of chemicals such as trace metals, hydrocarbons, radionuclides, or organophosphorus compounds, but also as a potential long-term secondary source of pollution. Scavenging of pollutants can be reversible due to several factors, including diagenetic changes, bioturbation, weather events or water management actions (Ouddane et al., 2018), but major transport of pollutants from estuaries onto the continental shelf probably occurs only during floods and storms (Ridgway and Shimmield, 2002). Furthermore, coastal areas are also affected by the impact of ongoing climate change and, in particular, sea-level rise (O´Shea et al., 2018).

The multidisciplinary study of sediment cores has been extensively used to reconstruct the recent environmental transformation of coastal areas (Baptista Neto, 2017; Polovodova Asteman et al., 2015; Ruiz-Fernández et al., 2012, 2016; Sreenivasulu et al., 2017). As sediments preserve a valuable fingerprint of natural events and human impacts, their records provide information useful for reconstructing contamination histories and trends, and for facilitating long-term risk assessment and sustainable management of estuaries (Birch et al., 2013). In many countries, restrictions on waste dumping and wastewater discharges during the past decades have significantly reduced the contaminant loads that enter the estuarine environment (Kennish, 2002), and ameliorated sediment quality (Heim and Schwarzbauer, 2013).

The Bilbao estuary (N Spain) offers a representative example of a historically contaminated waterway that is undergoing significant environmental improvement

(Cajaraville et al., 2016; García-Barcina, 2006; Leorri et al., 2008). However, large amounts of highly contaminated sediments remain stored in the estuarine bottom (Cearreta et al., 2000, 2002), mostly covered by a layer of cleaner materials that varies in thickness (Irabien et al., 2018). The widespread influence of human activities extends outside this estuary, as evidenced by areas of metal accumulation observed on the continental shelf, which are associated to disposal sites for blast furnace slags and dredged sediments (Legorburu et al., 2013), and the anthropogenic beachrock materials that emerge eastward of, and adjacent to, its mouth (Arrieta et al., 2017).

Previous studies developed in the Bilbao estuary using sediment cores have been focused on the historically contaminated deposits that cover the bottom of the estuarine channel (Cearreta et al., 2000, 2002; Cundy et al., 2003). Results reveal that vertical distribution of heavy metals and radionuclides is largely controlled by anthropogenic activities (inputs of mining and industrial wastes, dredging operations, etc). The human influence in such degraded areas is so pervasive that can mask the potential effects caused by other factors such as historical floods, which is thus a critical knowledge gap since extreme natural events are considered to be major threatening processes affecting the health and condition of estuaries and deltas (United Nations, 2017).

This is the first work to examine the recent sedimentary record at a small coastal embayment located at the estuary mouth (inner Abra of Bilbao bay; Figure 1) that, in principle, is less prone to local anthropogenic disturbances than the artificially channelized sections upstream. A multidisciplinary approach that includes geochemical (Pb, Zn and Cd), micropaleontological (benthic foraminifera), and isotopic (^{210}Pb, ^{137}Cs) proxies has been applied with the main aims of i) providing information about its contamination status and the influence of changing socio-economic trends, under the hypothesis that sewage pollution abatement measures taken by local authorities, the industrial crisis and the perceived shift of Bilbao city from a manufacturing to a service economy have contributed to the reduction of metal loads from the estuary; and ii)

drawing attention to the effects of extreme natural events, inherently difficult to prevent, in the sedimentary deposits of historically industrialised coastal areas..

2. Study area and background

The Bilbao estuary is a small mesotidal system located in the Basque Country (43º23´-43º14´N, 3º07¨-2º55´), on the northern Spanish coast (Figure 1). Since the first iron and steel factory started to process local ores on reclaimed salt marshes in 1854, this waterway has been the core of economic and social growth of the Bilbao Metropolitan Area (about 900,000 inhabitants in 2019). Unfortunately, urban and industrial expansion took place in the absence of an appropriate framework for sustainable development, so activities such as extensive land reclamation, multiple works to ensure navigability and port activities, uncontrolled discharges of huge amounts of untreated wastes (derived from the exploitation of local Fe ores, a wide array of industrial activities, and urban areas), and continuous dredging turned it into a largely artificial and contaminated system where two main areas can be distinguished.

The upper part is formed by a narrow (50–150 m wide), shallow (4–10 m depth) and highly stratified channel (about 15 km long) surrounded by a dense urban and industrial network, which was described in the 1970s as a navigable sewer running through one of the most polluted cities of the world (Woodworth, 2007). The lower reaches are occupied by a funnel-shaped coastal embayment known as the Abra of Bilbao, with a total area of about 30 km^2, maximum depth of 30 m and width of about 4 km (Mestres et al., 2014). It contains 95% of the total water of the estuary (Butrón et al., 2009). In the late 1800s, two breakwaters were built in Santurtzi and Algorta (Figure 1) to construct an external port, dividing the bay in two main zones: the outer Abra (where most port activities take place today) and the inner Abra (area of interest of this study). This infrastructure caused a significant change in the system hydrodynamics, preventing marine sands from entering the inner Abra, and thus favouring muddy sedimentation. Therefore, human-induced processes have not only altered the original

138 morphological features of the entire estuary but also the sedimentary regime (Saiz-
139 Salinas and Urkiaga-Alberdi, 1999). As a consequence, the sandy deposits of the Las
140 Arenas beach (Figure 1) almost disappeared, and reinforcement works were carried
141 out in the first decade of the 1900s to prevent further erosion. Subsequently, the
142 construction of port facilities such as the moorings of the Real Club Marítimo (1950s),
143 the new marina of Getxo (1999), and jetties for large cruise ships (2006 and 2012)
144 reduced the inner Abra bay to its current size (about 2 km^2).

145 Recent evolution of the environmental quality of the estuarine sediments from the
146 metropolitan area of Bilbao has been extensively documented (e.g. Bartolomé et al.,
147 2006; Fdez-Ortiz de Vallejuelo et al., 2010; Irabien et al., 2018; Leorri et al., 2008;
148 Prieto et al., 2008; Saiz-Salinas and González-Oreja, 1998; Seebold et al., 1982), but
149 much less attention has been paid to the inner bay deposits. However, previous studies
150 have detected elevated concentrations of metals in sediments from this area (Guerrero
151 Pérez et al., 1988; Swindlehurst and Johnston, 1991), which can exert a potential risk
152 to the environment (Belzunce et al., 2001). In 2014, heightened contents of metals
153 (higher than those found in 2009, 2010 and 2011) were attributed to the construction of
154 a new jetty for long tourist cruise liners in 2012 (Rodriguez-Iruretagoiena et al., 2016).
155 This work extends the study of sediment cores to this coastal embayment, providing
156 essential information to test potential differences between the sedimentary records
157 from areas with significantly different hydrodynamic and developmental conditions
158 within a historically industrialised estuarine system.

159 **3. Materials and methods**

160 3.1. Sampling

161 Six sediment cores (between 50 and 69 cm length) were collected in September
162 2015, using a hammer corer (10 cm internal diameter) operated by scuba divers, from
163 two transects of the inner Abra (two replicates at each sampling site; Figure 1, Table

1). All cores were described, photographed and X-radiographed before slicing into 1 cm sections.

3.2. Sediment geochemistry

Sediments for geochemical analysis were sieved through a 2 mm mesh, oven dried at 45 ºC and mechanically homogenised in an agate mortar and pestle. Elemental concentrations were analysed in Activation Laboratories Ltd. (Actlabs, Ontario, Canada) by Inductively Coupled Plasma-Mass Spectrometry (ICP-MS) after near total digestion using hydrofluoric, nitric, perchloric and hydrochloric acids. Lowest detection limits were 0.1 mg kg^{-1} for Cd and Pb, and 1 mg kg^{-1} for Zn.

The effect range-median (ERM) approach proposed by Long et al. (1995) was applied to assess the potential toxicological significance of the determined metal contents. These reference values (220 mg kg^{-1} for Pb, 410 for Zn and 9.6 for Cd) are derived from compiled biological toxicity assays and represent concentrations above which frequent adverse effects on benthic organisms are expected.

3.3. Benthic microfauna

Samples for foraminiferal analysis were sieved through a 63 μm mesh and washed with tap water to remove clay- and silt-size (mud) fractions. Samples were dried at 50 ºC and weighed to determine grain size percentages (sand and mud). Foraminiferal tests were concentrated by flotation in trichloroethylene as described by Murray (2006) and the heavy residue was examined for possible unfloated shells. Tests were picked until a representative sample of > 300 individuals was obtained. When foraminifera were scarce, all the available tests were extracted and examined under a stereoscopic binocular microscope using reflected light. Abundance is expressed as number of foraminiferal tests per 15 g of sediment. Abundance results were grouped (very low, low, moderate, high and very high) following the quantification of absolute and relative abundances of foraminiferal tests and species for estuaries in northern Spain

190 presented in García-Artola et al. (2016). In total, 185 samples and more than 38,680
191 foraminiferal tests were studied.

192 3.4. Radiometric analysis

193 Activities of ^{210}Pb, ^{226}Ra and ^{137}Cs in cores Abra1 and Abra4 were analysed by
194 gamma spectrometry, using a low-background high purity germanium (HPGe) detector,
195 in the University of Cantabria. Sediment samples were homogenised, sieved (< 0.5
196 mm), hermetically sealed and stored for at least 30 days to ensure secular equilibrium
197 between ^{226}Ra, ^{222}Rn and the short-lived daughter nuclides of the latter. The
198 methodology used for these cores is described in Cearreta et al. (2013) and particular
199 details can be found in Alvarez-Iglesias et al. (2007). For sediment cores Abra2, Abra3,
200 Abra5 and Abra6, ^{210}Pb activities were determined through its radioactive descendent
201 ^{210}Pb by alpha spectrometry (Ortec-Ametek Alpha Ensemble), and ^{226}Ra and ^{137}Cs
202 were measured by high-resolution, low-background gamma spectrometry (Ortec-
203 Ametek HPGe well detector) in the Servicio Académico de Fechado at National
204 Autonomous University of Mexico, following Ruiz-Fernández and Hillaire-Marcel
205 (2009).

206 Although all cores showed a down-core decrease in activity, none of the profiles
207 were clearly exponential, indicating that accumulation rates were not constant.
208 Therefore, age models and accumulation rates (sediment accumulation rate, SAR, and
209 mass accumulation rates, MAR) were estimated, in most cases, through the Constant
210 Flux (CF) model (Sánchez-Cabeza and Ruiz-Fernández, 2012), which assumes a
211 constant ^{210}Pb flux but variable sedimentation rates. When this was not possible, the
212 CFCS model (which additionally assumes constant sedimentation) was used. Although
213 the CF model requires knowledge of the total $^{210}Pb_{ex}$ inventory in the core, except for
214 the Abra2 core, all cores showed ^{210}Pb-^{226}Ra disequilibrium and ^{137}Cs activities in the
215 bottom sections, indicating that $^{210}Pb_{ex}$ inventories were incomplete.

216 **4. Results and discussion**

The full datasets of geochemical, microfaunal and radiometric data obtained in this work are provided in Appendices A, B, and C respectively. Contents of Pb, Zn and Cd in almost all sediment samples are far in excess of those provided by Rodriguez et al. (2006) as regional background values (see Table 1), confirming the historical environmental impact exerted by human activities in this area. In the most enriched samples concentrations of Pb and Cd exceed by two order of magnitude these reference values, while levels of Zn are more than one order of magnitude higher.

4.1. Transect A (cores Abra1, Abra2 and Abra3)

The vertical distribution of all variables is broadly similar (Figure 2), allowing three different depth intervals (DIs) to be distinguished (Table 1). Sediments collected below ~45 cm depth (DI1) show extremely high contents of metals and are particularly enriched in Pb. In local pre-industrial samples (Cearreta et al., 2000), and in almost all surface sediments collected throughout the environmental monitoring programme developed in the estuarine channel from 1997 to 2017 (Cearreta et al., 2000; Irabien et al., 2018; Leorri et al., 2008), Pb contents are distinctly lower than Zn concentrations (Pb/Zn < 0.35 and 0.5 respectively). Conversely, as observed in some samples of contaminated sediments buried upstream of the Abra (Irabien et al., 2018), in DI1 Pb levels are similar or even higher than those of Zn (0.8 < Pb/Zn < 1.6), showing increased Pb contamination in the past.

The muddy DI1 interval (sand content median 6%) contains a very low foraminiferal abundance (32 tests/15 g) dominated by *Ammonia tepida* (median 28%), *Cibicidoides lobatulus* (18%), *Rosalina irregularis* (13%), *Bulimina gibba* (11%), *Haynesina germanica* (6%) and *Quinqueloculina seminula* (6%). Species number is low (7), marine foraminiferal content is high (62%), and hyaline tests are highly dominant (91%), with a significant contribution from porcellaneous species (8%).

DI2, from ~45 to ~25 cm depth, is characterised by the occurrence of significant grain-size changes (sandy peaks), a decrease in metal concentrations (minimum

contents are at least one order of magnitude lower than those found in DI1), and Pb/Zn ratios ranging from 0.55 to 0.8. This sandy mud interval (sand content 20%) shows the dominant presence of *A. tepida* (26%), *R. irregularis* (24%), *H. germanica* (16%) and *C. lobatulus* (15%). The assemblage is composed of a moderate number of foraminifera (235 tests/15 g), species (15), marine taxa (53%), and very high hyaline tests (94%) with a lower porcellaneous content than DI1 (5%).

The $^{210}Pb_{ex}$ depth profiles in the three cores exhibit a general declining trend with depth, but in the DI2 interval, $^{210}Pb_{ex}$ activities were small or zero. Although this could suggest that DI2 was deposited more than 100 years ago, the occurrence of higher $^{210}Pb_{ex}$ activities in sediment below this level (at interval DI1) in cores Abra1 and Abra3 (the lower part of the Abra2 core was not recovered), plus the presence of ^{137}Cs in both intervals (DI1 and DI2), indicate that deposition occurred after 1952. The small or zero $^{210}Pb_{ex}$ activity in this interval was probably caused by a sedimentary event transporting particles, most likely eroded catchment soils, in ^{210}Pb-^{226}Ra equilibrium.

The Abra1 core showed a broad equilibrium interval (26–42 cm). Its missing inventory was calculated by using the accumulation rate method (Sánchez-Cabeza and Ruiz-Fernández, 2012) by linear regression, and the date of this interval was compatible with the Bilbao catastrophic floods of 1983. Assuming that all equilibrium or dilution intervals in Abra2 and Abra3 were caused by the same event, the reference date method was used to calculate the missing inventories. The dramatic increase in mass accumulation rates, and textural and compositional changes, confirm that DI2 corresponds to an extraordinary sedimentary event. This event is identified as the floods of August 1983, the worst natural catastrophe in the Basque Country's recent history, during which significant amounts of coarse-grained and cleaner sediments were transported to the inner Abra. Although it certainly had a dramatic impact over the whole region, this is the first time that evidences are found in the estuarine sedimentary record.

271 Finally, the transition to the upper core zone (DI3) is marked by a significant
272 increase in metal concentrations (Figure 2), which declines towards the more recent
273 sediments. Contrary to the concentrations measured in DI1, Pb levels are at least half
274 that of Zn (Pb/Zn < 0.5), which approaches Pb/Zn ratios determined upstream in
275 surface estuarine channel materials monitored from 1997 to 2017, and reflects a
276 change in anthropogenic sources over time. Sediments in DI3 return to dominantly mud
277 (sand content 6%), and a moderate foraminiferal density (210 tests/15 g) and species
278 number (17) are observed. Foraminiferal species are represented mainly by *A. tepida*
279 (46%), *R. irregularis* (11%), *C. lobatulus* (10%), *Eggerelloides scaber* (6%) and *B.*
280 *gibba* (5%). Marine foraminifera (44%) are less abundant than estuarine forms, and
281 hyaline tests continue to be highly dominant (91%) with distinct agglutinated test
282 abundance (6%).

283 4.2. Transect B (cores Abra4, Abra5 and Abra6)

284 Cores Abra5 and Abra6 are almost exclusively composed of fine-grained materials
285 (3% sand), while core Abra4 exhibits a noticeably high sand content below 30 cm
286 depth (Figure 3).

287 In the basal zone of core Abra4, maximum values of MAR are observed (~40 cm
288 depth), $^{210}Pb_{ex}$ activities remain constant and fairly low (although no zero values are
289 reached), and Pb/Zn ratios range from 0.6 to 0.8. Micropaleontological features of this
290 sandy mud interval (sand content 37%) exhibit dominant *A. tepida* (36%,), *C. lobatulus*
291 (15%), *H. germanica* (6%) and *R. irregularis* (4%), a moderate number of foraminifera
292 (340 tests/15 g), species (20), and marine taxa (46%), and a high abundance of hyaline
293 tests (87%) with secondary porcellaneous forms (12%). Despite being less evident, all
294 these characteristics strongly resemble the DI2 interval in the cores of transect A
295 (Figure 2), reflecting the same extraordinary sedimentary event. Likewise, the upper
296 part of the core is broadly similar to DI3 of transect A, with the lowest values of metals
297 measured in the near surface samples, Pb/Zn ratios < 0.5, an almost identical

298 microfaunal assemblage, and $^{210}Pb_{ex}$ activities decreasing with depth, indicating regular
299 sedimentation.

300 Sediments from core Abra5 show a rather homogenous granulometric distribution
301 and increasing concentrations of metals with depth (Figure 3). In fact, bottom samples
302 exhibit the highest concentrations of Cd found in this work. Significant peaks of this
303 element can also be observed in all cores from transect A (Figure 2), both in down-core
304 sediments (DI1), where Pb/Zn ratios are above 0.8, and in upper core samples (DI3),
305 where Pb/Zn values are below 0.5. As Pb/Zn ratios in core Abra5 range from 0.4 to 0.3,
306 they are compatible with the upper interval DI3 from transect A, suggesting recent
307 deposition and higher sedimentation rates. Moreover, $^{210}Pb_{ex}$ activities display an
308 almost constant and erratic profile (Figure 3). Although constant sedimentation cannot
309 be assumed in any of the Abra cores, the CFCS model (Sánchez-Cabeza and Ruiz-
310 Fernández, 2012) provides a rather young bottom age (1999 $\pm$ 8), confirming that
311 sediment accumulation is high, but it cannot be estimated because regressions are not
312 significant. The Cd peak in bottom samples is in good agreement with the maximum
313 found in core Abra3 at about 15 cm, and dates to the late 1990s (1998 $\pm$ 1).

314 Sediments from the entire Abra6 core likely belong to interval DI3, given their
315 relatively low metal content, decreasing towards the surface (Figure 3), and low Pb/Zn
316 ratios (< 0.5). CFCS dating of Abra6 yielded a maximum core age of 1994 $\pm$ 3. The
317 vertical profile of $^{210}Pb_{ex}$ activities reveals two recent episodes of sediment dilution, in
318 the early 2000s and 2008.

319 Finally, microfossil assemblages in Abra4 (upper muddy interval), Abra5 and Abra6
320 also resembled interval DI3 of the cores from transect A. Foraminiferal content (292
321 tests/15 g) and species number (19) are moderate. Species *A. tepida* (50%), *B. gibba*
322 (6%), *R. irregularis* (6%), *E. scaber* (5%) and *C. lobatulus* (4%) are the most important
323 forms. Marine foraminifera (38%) are secondary to prevailing estuarine taxa. Hyaline

tests are highly dominant (91%), followed by similar agglutinated and porcellaneous contents.

4.3. Historical interpretation and environmental assessment

Based on the combined analysis of the results from geochemical, microfaunal and radiometric proxies, it is possible to distinguish three different environmental zones within the recent sedimentary record of the inner Abra bay. The first zone is represented by interval DI1 (below about 45-50 cm depth), which is only identified in transect A cores (Figure 2). These muddy sediments witness highly degraded environmental conditions during past times of unsustainable development. They are so enriched in Pb that concentrations of this metal in most samples exceed the upper threshold value established for “non-hazardous sediments” (1000 mg kg^{-1}), according to the Spanish framework for the characterisation of dredged materials (Buceta et al., 2015). Therefore, further studies should be carried out to determine if these sediments should be handled as hazardous wastes or as highly contaminated materials, which is of particular importance to dredging activities. Moreover, the sediments also exhibit high levels of Cd and Zn, which exceed the ERM values proposed by Long et al. (1995). Highly contaminated sediments with similar metal concentrations have been observed in cores from intertidal flats a few km upstream (Irabien et al., 2018), confirming the role of the whole estuarine system as a sink for industrial wastes. The co-occurrence of Pb and Cd indicates that they may share a common source related to the local steel mill industry (Legorburu et al., 2013). Benthic foraminifera are very scarce in this basal zone and are composed of a mixture of limited marine (mainly *C. lobatulus*, *R. irregularis* and *B. gibba*) and estuarine (*A. tepida*) species.

The following interval (DI2) can be recognised in cores Abra1, Abra2, Abra3 and Abra4 (Figures 2 and 3). It is characterised by the accumulation of sandy layers with low concentrations of metals intercalated with muddy sediments showing variable contamination degrees. Although decreased values of metals in populated and

industrialised regions are often a consequence of a decline in anthropogenic inputs, data from the isotopic analysis indicate that in this case they are related to the deposition of materials remobilised during the extreme floods that affected the Basque Country in August 1983 (Cearreta et al., 2017). This emphasises the need to address a multidisciplinary approach to reliably interpreting the recent sedimentary record in coastal areas, where natural disturbances often interplay with a wide variety of human activities.

The floods of 1983 were unprecedented, as the rainfall during three days (August 24, 25 and 26) equalled the monthly maximum recorded in 125 years (Instituto Geológico y Minero de España, 1986). In just 24 h (from 9:00 AM on Friday 26 to 9:00 AM on Saturday 27) rainfall was about 500 mm. River flow, that likely exceeded the 1000-year return period, caused generalised flooding throughout the region (especially in the estuarine areas, where the maximum flow coincided with high tide), 39 fatalities, and economic losses of more than €800 million (Ocio et al., 2015). This extreme weather event was the consequence of the interaction of warm advection through the Mediterranean with a polar air mass in high layers, which generated a mesoscale convective system responsible for the unusually abundant and intense rainfall (Egaña and Gaztelumendi, 2018). Known in Spain as “cold drop”, this phenomenon appears to be the major regional flood threat (Ocio et al., 2015). In fact, river and flash flooding exacerbated by tidal variations has been identified as the main natural hazard that the city of Bilbao has periodically faced throughout its centennial history (Adán de Yarza, 1892; Landa Méndez, 2014). Unfortunately, convective phenomena in the Basque Country are predicted to increase in the future as a result of global warming, leading to increased risk of extreme rainfall events and floods (Benito et al., 2005).

The local hydrodynamic motion in the inner Abra bay is mostly tidally-induced, and the wind-wave contribution to currents is assumed to be negligible (Grifoll et al., 2009). The mean freshwater outflow is relatively low and, for larger river flows, the plume exits the estuary along the right bank and stays attached to the eastern coast (Mestres et al.,

2014). However, tidal currents are diverted by the local morphology, the human-made infrastructure, and terrestrial rotation, resulting in a clockwise current during ebb tide (and anticlockwise during flood tide) (Lugaresaresti Bilbao, 1994) that contributes to the relocation of sediments during extreme meteorological events such as floods and storms.

Benthic foraminifera of the sandier DI2 interval exhibit a mixture of estuarine (mainly *A. tepida* and *H. germanica*) and marine hyaline species (*C. lobatulus* and *R. irregularis*). This assemblage highly resembles the foraminiferal species composition of the sandy Holocene sediments that characterised the lower Bilbao estuary (Leorri and Cearreta, 2004), suggesting that could be the main source of the sandy sediments accumulated in the bay during the catastrophic flood event of 1983. However, the peak metal values found at about 40–45 cm depth in the Abra3 core, which broadly resemble increased $^{210}Pb_{ex}$ levels, are more likely related to the deposition of remobilised contaminated sediments.

Turbulent flow conditions, which remove considerable volumes of sediment and associated contaminants, can expose anoxic sediments to oxic conditions, affecting the release and bioavailability of pollutants (Eggleton and Thomas, 2004). The evidences of sediment mixing in DI2 (granulometric and compositional changes, sharp decrease in $^{210}Pb_{ex}$ activities, changes in foraminiferal assemblages) confirm that disturbances caused by extreme weather events can compound anthropogenic impacts in coastal and marine areas (Ralston et al., 2013). Similarly, Ruiz and Saiz-Salinas (1999) found significant variations in metal concentrations in sediments and bivalves from the Bilbao estuary which were related to a drought in 1989–1990.

The upper core interval (DI3) represents the post-1983 period (Figures 2 and 3). Although the general trend in metal concentrations decreases towards more recent sediments, high concentrations still remain in the lower part (except in core Abra6, where accumulated materials are remarkably younger). This is not surprising, given that the significant improvement of the chemical quality of the surface sediments took

407 place in the Bilbao estuary from 2000–2003 onwards (Leorri et al., 2008). Except in
408 core Abra5, where all samples exceed the ERM value for Zn, in the other studied cores
409 there is a topmost layer of sediments whose concentrations of metals are below the
410 ERM values. Similarly to that observed in the estuarine channel area (Irabien et al.,
411 2018), thickness of this layer of "cleaner" sediments ranges between 1 cm (Abra3) and
412 21 cm (Abra6), Moreover, this recent muddy interval exhibits the highest abundance of
413 estuarine foraminifera (mainly *A. tepida*) over marine species (*R. irregularis*, *C.*
414 *lobatulus, E. scaber* and *B. gibba*), making it qualitatively similar to interval DI1 but with
415 much higher foraminiferal contents, indicative of the improvement of environmental
416 conditions for survival. Therefore, future management actions (dredging operations,
417 monitoring of natural recovery) should take into account not only the historical legacy of
418 contaminated sites, but also the current impacts (physico-chemical, biological,
419 ecological) of the regeneration process.
420

421 **5. Conclusions**

422 Our results indicate that the study of sedimentary deposits from historically
423 industrialised coastal areas is a complex task that demands a multidisciplinary
424 approach. The combination of geochemical, micropaleontological and isotopic proxies
425 applied to sediment cores from the inner Abra of Bilbao (northern Spain) has allowed
426 us:

427 - To correlate data obtained from cores representing different time spans in order to
428 integrate them in an accurate spatial and historical framework;

429 - To assess the environmental quality evolution of the sedimentary deposits.
430 Sediments with significantly high concentrations of metals are somewhat hidden below
431 a thin layer (< 22 cm) of "cleaner", recently deposited sediments that has accumulated
432 since anthropogenic discharges have substantially decreased. Therefore, and even if
433 regeneration processes like this are still in progress, their accurate characterisation and

risk assessment continue to challenge the current and future management of many industrialised and populated coastal areas.

- To discriminate anthropogenic impacts from those related to an extreme weather event (as the Bilbao historical floods of 1983);

- To confirm relocation of sediments related to this historical episode of floods. This highlights the need to improve our understanding of the potential impact that extreme weather events, already on the increase due to current climate change, can exert on contaminated sites, since they can remobilise older sediments, promoting the release of contaminants that had been sequestered, and hindering and even reverting environmental improvement efforts.

Acknowledgements: This research was funded by Spanish MINECO (CGL2013-41083-P and RTI2018-095678-B-C21, MCIU/AEI/FEDER, UE), UPV/EHU (UFI11/09) and EJ/GV (IT976-16) projects. Microfossil samples of cores Abra1, Abra4 and Abra6 were prepared and analysed initially by I. Kortabitarte and A. González-Lanchas. L.H. Pérez-Bernal (UNAM) contributed to ^{210}Pb and sediment characterisation analyses. This is contribution 48 of the Geo-Q Zentroa Research Unit (Joaquín Gómez de Llarena Laboratory). The authors thank the two anonymous reviewers for their comments, critical reviews, and constructive suggestions. Dr Damiá Barceló (Co-Editor-in-Chief) is warmly acknowledged for his helpful decisions and encouragement as this paper was evolving.

References

Adán de Yarza, R. 1892. Descripción Física y Geológica de la provincia de Vizcaya. Memorias de la Comisión del Mapa Geológico de España, 192 pp.

460 Alvarez-Iglesias, P., Quintana, B., Rubio, B., Perez-Arlucea, M. 2007. Sedimentation
461 rates and trace metal input history in intertidal sediments from San Simón bay
462 (Ría de Vigo, NW Spain) derived from ^{210}Pb and ^{137}Cs chronology. J. Environ.
463 Radioact. 98, 229-250.

464 Arrieta, N., Iturregui, A., Martínez-Azkaraz, I., Murelaga, X., Baceta, J.I., de Diego, A.,
465 Olazabal, M.A., Madariaga, J.M. 2017. Characterization of ferruginous cements
466 related to weathering of slag in a temperate anthorpogenic beachrock. Sci. Total
467 Environ. 581-582, 49-65.

468 Baptista Neto, J.A., Ferreira Barreto, C., Guterres Vilela, C., Monteiro da Fonseca, E.,
469 Vaz Melo, G., Monica Barth, O. 2017. Environmental change in Guanabara Bay,
470 SE Brazil, based in microfaunal, pollen and geochemical proxies in sedimentary
471 cores. Ocean Coast. Manag. 143, 4-15.

472 Bartolomé, L., Tueros, I., Cortazar, E., Raposo, J.C., Sanz, J., Zuloaga, O., de Diego,
473 A., Etxebarria, N., Fernandez, L.A., Madariaga, J.M. 2006. Distribution of trace
474 organic contaminants and total mercury in sediments from the Bilbao and Urdaibai
475 Estuaries (Bay of Biscay). Mar. Pollut. Bull. 52, 1111–1117.

476 Belzunce, M.J., Solaun, O., Franco, J., Valencia, V., Borja, A. 2001. Accumulation of
477 organic matter, heavy metals and organic compounds in surface sediments along
478 the Nervión estuary (northern Spain). Mar. Pollut. Bull. 42, 1407-1411.

479 Benito, G., Barriendos, M., Lasat, C., Machado, M., Thorndycraft, V.R. 2005. Impactos
480 sobre los riesgos naturales de origen climático. In: Evaluación preliminar de los
481 impactos en España por efecto del Cambio Climático, 527-548. Ministerio de
482 Medio Ambiente.

483 Birch, G.F., Chang, C.H., Lee, J.H., Churchill, L.J. 2013. The use of vintage surficial
484 sediment data and sedimentary cores to determine past and future trends in

485 estuarine metal contamination (Sidney estuary, Australia). Sci. Total Env. 454-
486 455, 542-561.
487 Bowron, T., Neatt, N., van Proosdij, D., Lundhom, J., Graham, J. 2009. Macro-tidal salt
488 marsh ecosystem response to culvert expansion. Restor. Ecol. 19, 307-322.
489 Buceta, J.L., Lloret, A., Antequera, M., Obispo, R., Sierra, J., Martínez-Gil, M. 2015.
490 Nuevo marco para la caracterización y clasificación del material dragado en
491 España. Ribagua 2, 105-115.
492 Butrón, A. Iriarte, A., Madariaga, I. 2009. Size-fractionated phytoplankton biomass,
493 primary production and respiration in the Nervión-Ibaizabal estuary: A comparison
494 with other nearshore coastal and estuarine ecosystems from the Bay of Biscay.
495 Cont. Shelf Res. 29, 1088-1102.
496 Cajaraville, M.P., Orive, E., Villate, F., Laza-Martínez, A., Uriarte, I., Garmendia, L.,
497 Ortiz-Zarragoitia, M., Seoane, S., Iriarte, A., Marigómez, I. 2016. Health status of
498 the Bilbao estuary: A review of data from a multidisciplinary approach. Estuar.
499 Coast. Shelf Sci. 179, 124-134.
500 Cearreta, A., Irabien, M.J., Leorri, E., Yusta, I., Croudace, I.W., Cundy, A.B. 2000.
501 Recent Anthropogenic Impacts on the Bilbao Estuary, Northern Spain:
502 Geochemical and Microfaunal Evidence. Estuar. Coast. Shelf S. 50, 571-592.
503 Cearreta, A., Irabien, M.J., Ulibarri, I., Yusta, I., Croudace, I.W., Cundy, A.B. 2002.
504 Environmental transformation of the Bilbao estuary, N. Spain: microfaunal and
505 geochemical proxies in the recent sedimentary record. Mar. Pollut. Bull. 44, 487-
506 503.
507 Cearreta, A., García-Artola, A., Leorri, E., Irabien, M.J., Masque, P. 2013. Recent
508 environmental evolution of regenerated salt marshes in the southern Bay of
509 Biscay: Anthropogenic evidences in their sedimentary record. J. Mar. Syst. 109–
510 110 Supplement, S203-S212.

511 Cearreta, A., Irabien, M.J., Gómez-Arozamena, J., Kortabitarte, I., González-Lanchas,
512 A. 2017. El registro geológico antropoceno en el Abra de Bilbao: evidencias de su
513 historia natural y humana. Geogaceta 61, 11-14.

514 Egaña, J., Gaztelumendi, S. 2018. A study of meteorological conditions during the
515 historical August 1983 Basque Country floods. EMS Annual Meeting Abstracts
516 15, EMS2018-636.

517 Eggleton, J., Thomas, K.V. 2004. A review of factors affecting the release and
518 bioavailability of contaminants during sediment disturbance events. Environ. Inter.
519 30, 973-980.

520 Fdez-Ortiz de Vallejuelo, S., Arana, G., de Diego, A., Madariaga, J.M. 2010. Risk
521 assessment of trace metals in sediments: the case of the estuary of the Nerbioi-
522 Ibaizabal river (Basque Country). J. Hazard. Wastes 1-3, 565-573.

523 García-Artola, A., Cearreta, A., Irabien, M.J., Leorri, E., Sánchez-Cabeza, J.A.,
524 Corbett, D.R. 2016. Agricultural fingerprints in salt-marsh sediments and
525 adaptation to sea-level rise in the eastern Cantabrian coast (N. Spain). Estuar.
526 Coast. Shelf Sci. 171, 66–76.

527 Garcia-Barcina, J.M., González-Oreja, J.A., de la Sota, A. 2006. Assessing the
528 improvement of the Bilbao estuary water quality in response to pollution abatement
529 measures. Water Res. 40, 951-960.

530 Grifoll, M., Fontán, A., Ferre, L., Mader, J., González, M., Espino, M. 2009. 3D
531 hydrodynamic characterization of a meso-tidal estuary: the case of Bilbao
532 (northern Spain). Coast. Eng. 55, 907-918.

533 Guerrero Pérez, J., Rodriguez Puente, C., Jornet Sancho, A. 1988. Estudio de metales
534 pesados en aguas y sedimentos superficiales de las costas gallegas y
535 cantábricas, Informes Técnicos del Instituto Español de Oceanografía, 64. 16 p.

536 Heim, S., Schwarzbauer, J. 2013. Pollution history revealed by sedimentary records: a
537 review. Environ. Chem. Let 11, 255-270.

Instituto Geológico y Minero de España. 1986. Estudio geológico para la previsión de riesgos por inundaciones en el País Vasco (Alava y Vizcaya) y condado de Treviño. Serie Geología Ambiental, 73 pp.

Irabien, M.J., Cearreta, A., Serrano, H., Villasante-Marcos, V. 2018. Environmental regeneration processes in the Anthropocene: the Bilbao estuary case (northern Spain). Mar. Pollut. Bull. 135, 977-987.

Kennish, M.J. 2002. Environmental threats and environmental future of the estuaries. Environ. Conserv. 29, 78-107.

Landa Méndez, N. 2014. Adaptation to urban floods by planning and design. Guidelines for an adaptive management to urban floods and storm water use taking as a case study the City of Bilbao. Degree Project, KTH Royal Institute of Technology, 74 pp. http://www.diva-portal.org/smash/get/diva2:727431/FULLTEXT01 (last access June 2019)

Legorburu, I., Galparsoro, I., Larreta, J., Rodriguez, J.G., Borja, A. 2013. Spatial distribution of metal accumulation areas on the continental shelf of the Basque Country (Bay of Biscay): A GIS-based project. Estuar. Coast. Shelf Sci. 134, 162-173.

Leorri, E., Cearreta, A. 2004. Holocene environmental development of the Bilbao estuary, northern Spain: sequence stratigraphy and foraminiferal interpretation. Mar. Micropal. 51, 75-94.

Leorri, E., Cearreta, A., Irabien, M.J., Yusta, I. 2008. Geochemical and microfaunal proxies to assess environmental quality conditions during the recovery process of a heavily polluted estuary: The Bilbao estuary case (N. Spain). Sci. Total Environ. 396, 12-27.

Li, X., Bellerby, R., Craft, C., Widney, S.E. 2018. Coastal wetland loss, consequences and challenges for restoration. Anthropocene Coasts 1, 1-15.

564 Long, E.R., MacDonald, D.D., Smith, S.L., Calder, F.D. 1995. Incidence of adverse
565 biological effects within ranges of chemical concentrations in marine and estuarine
566 sediments. Environ. Manage. 19, 81–97.

567 Lugaresaresti Bilbao, J.I. 1994. Aspectos del clima maritime y morfodinámica en el
568 Puerto exterior de Bilbao (Shoreface morphodynamics in the Abra Bay of Bilbao,
569 Basque Country). Kobie 22, 23-32.

570 Mestres, M., Sierra, J.P., Mösso, C., Sánchez-Arcilla, A., Hernáez, M. 2014. Numerical
571 assessment of the dispersion of overspilled sediment from a dredge barge and its
572 sensitivity to various parameters. Mar. Poll. Bull. 79, 225-235.

573 Mossman, H.L., Davy, A.J., Grant, A. 2012. Does managed coastal realignment create
574 saltmarshes with “equivalent biological characteristics” to natural references sites?
575 J. Appl. Ecol. 49, 1446-1456.

576 Murray, J.W. 2006. Ecology and applications of benthic foraminifera. Cambridge
577 University Press, 426 pp.

578 Ocio, D., Stoker, C., Eraso, A., Cowpertwait, P. 2015. Regionalized extreme flows by
579 means of stochastic storm generation coupled with a distributed hydrological
580 model. The case of the Basque Country. E-proceedings of the 36th IAHR World
581 Congress.

582 O´Shea, F.T., Cundy, A.B., Spencer, K.L. 2018. The contaminant legacy from historic
583 coastal landfills and their potential as sources of diffuse pollution. Mar. Pollut. Bull.
584 128, 466-455.

585 Ouddane, B., Hamzeh, M., Daye, M. 2018 Implications of sulphide on trace metal
586 pollution mobility in sediment. In: Recent advances in environmental science from
587 the Euro-Mediterranean and surrounding regions, 19-22. Interdisciplinary Series
588 for Sustainable Development, Springer.

589 Polovodova Asteman, I., Hanslik, D., Nordberg, K. 2015. An almost completed
590 pollution-recovery cycle reflected by sediment geochemistry and benthic
591 foraminiferal assemblages in a Swedish-Norwegian Skagerrak fjord. Mar. Pollut.
592 Bull. 95, 126-140

593 Prieto, A., Zuloaga, O., Usobiaga, A., Bartolomé, L., Fernández, L. A., Etxebarria, N.,
594 Cipriain, E., Alonso, A. 2008. Levels and spatial distribution of inorganic and
595 organic contaminants in sediments along the Bilbao estuary. Mar. Pollut. Bull. 56,
596 2094-2099.

597 Ralston, D.K., Warner, J.C., Geyer, W.R., Wall, G.R. 2013. Sediment transport due to
598 extreme events: the Hudson River estuary after tropical storms Irene and Lee.
599 Geophys. Res. Lett. 40, 5452-5455.

600 Ridgway, J., Shimmield, G. 2002. Estuaries as repositories of historical contamination
601 and their impact on shelf seas. Estuar. Coast. Shelf Sci. 55, 903-928.

602 Robb, C.K. 2014. Assessing the impact of human activities on British Columbia
603 estuaries. Plos ONE 9, e99578.

604 Rodriguez, J.G., Tueros, I., Borja, A., Belzunce, M.J., Franco, J., Solaun, O., Valencia,
605 V., Zuazo, A. 2006. Maximum likelihood mixture estimation to determine metal
606 background values in estuarine and coastal sediments within the European Water
607 Framework Directive. Sci. Total Environ. 370, 278-293.

608 Rodriguez-Iruretagoiena, A., Elejoste, N., Gredilla, A., Fdez-Ortiz de Vallejuelo, S.,
609 Arana, G., Madariaga, J.M., de Diego, A. 2016. Occurrence and geographical
610 distribution of metals and metalloids in sediments of the Nerbioi-Ibaizabal estuary
611 (Bilbao, Basque Country). Mar. Chem. 185, 82-90.

612 Ruiz, J.M., Saiz-Salinas, J.I. 1999. Extreme variation in the concentrations of trace
613 metals in sediments and bivalves from the Bilbao estuary (Spain) caused by the
614 1989-90 drought. Mar. Environ. Res. 49, 1-11.

615 Ruiz-Fernández, A.C., Hillaire-Marcel, C. 2009. ^{210}Pb-derived ages for the
616 reconstruction of terrestrial contaminant history into the Mexican Pacific coast:
617 Potential and limitations. Mar. Pollut. Bull. 59, 134-145

618 Ruiz-Fernández, A.C., Sánchez-Cabeza, J.A., Alonso-Hernández, C. Martínez-
619 Herrera, V., Pérez-Bernal, L.H., Preda, M., Hillaire-Marcel, C., Gastaud, J.,
620 Quejido-Cabezas, A.J. 2012. Effects of land use change and sediment mobilization
621 on coastal contamination (Coatzacoalcos River, Mexico). Cont. Shelf Res. 37, 57–
622 65.

623 Ruiz-Fernández, A.C., Sánchez-Cabeza, J.A., Serrato de la Peña, J.L., Pérez Bernal,
624 L.H., Cearreta, A., Flores-Verdugo, F., Machain, M., Chamizo, E., García-Tenirio,
625 R., Queralt, I., Dunbar, R., Mucciarone, D., Diaz Asencio, M. 2016. Accretion rates
626 in coastal wetlands of the southeastern Gulf of California and their relationship with
627 sea-level rise. Holocene 26, 1126–1137.

628 Saiz-Salinas, J.I., González-Oreja, J.A. 1998. Coprostanol levels and organic
629 enrichment in sediments of the Bilbao estuary (north of Spain). Oceanol. Acta 21,
630 319-324.

631 Saiz-Salinas, J.I., Urkiaga-Alberdi, J. 1999. Faunal responses to turbidity in a man-
632 modified bay (Bilbao, Spain). Mar. Environ. Res. 47, 331-347.

633 Sánchez-Cabeza, J.A., Ruiz-Fernández, A.C. 2012. ^{210}Pb sediment radiochronology:
634 An integrated formulation and classification of dating models. Geochim.
635 Cosmochim Acta 82, 183-200.

636 Seebold, I., Labarta, C. Amigó, J.M. 1982. Heavy metals in the sediments of the Bilbao
637 estuary. In: Analytical Techniques in Enviromental Chemistry, 459-463. Pergamon
638 Press. Oxford.

639 Sreenivasulu, G., Jayaraju, N., Sundara Raja Reedy, B.C., Lakshmi Prasad, T.,
640 Nagalakshmi, K., Lakhsmanna, B. 2017. Foraminiferal research in coastal
641 ecosystems in India during the past decade: a review. Geo. Res. J. 13, 38-48.

642 Swindlehurst, R.J., Johnston, P.A. 1991. Severe heavy metal and PAH contamination
643 in Bilbao, Northern Spain. Greenpeace Technical Report, 19 p.

644 United Nations. 2017. First Global Integrated Marine Assessment. World Ocean
645 Assessment I. Cambridge University Press, 973 p.

646 Woodworth, P. 2007. The Basque country: a cultural history. Oxford University Press.

647 World Wildlife Foundation. 2015. Our ocean under pressure. In: Living Blue Planet
648 Report: Species, habitats and human well-being, 22-40.
649 https://www.wwf.or.jp/activities/data/20150831LBPT.pdf (last access June 2019)

650

651

652 Figure 1. Geographic location of the inner Abra of Bilbao, showing positions of the six
653 studied cores (Abra1, Abra2, Abra3, Abra4, Abra5 and Abra6).
654
655 Figure 2. Vertical distribution of sand content (%), total foraminiferal absolute
656 abundance (15 g of dry sediment), Pb, Zn and Cd (mg kg^{-1}), ^{210}Pb (Bq kg^{-1}) and mass
657 accumulation rates (MAR, kg m^2 y^{-1}) with depth in cores Abra1, Abra2 and Abra3.
658
659 Figure 3. Vertical distribution of sand content (%), total foraminiferal absolute
660 abundance (15 g of dry sediment), Pb, Zn and Cd (mg kg^{-1}) and ^{210}Pb (Bq kg^{-1}) with
661 depth in cores Abra4, Abra5 and Abra6. Mass accumulation rates (MAR, kg m^2 y^{-1}) are
662 included for core Abra4.
663
664 Table 1. Summary of lithological, geochemical and microfaunal data in the Abra cores.
665 The single value represents the median and those in parentheses give the range. Metal
666 values are expressed in mg kg^{-1}. As references for comparison, regional background
667 levels proposed by Rodriguez et al. (2006) are 31 mg kg^{-1} for Pb, 174 mg kg^{-1} for Zn,
668 and 0.24 mg kg^{-1} for Cd. Abundances of foraminifera are given in number of tests / 15 g
669 of dry sediment.
670

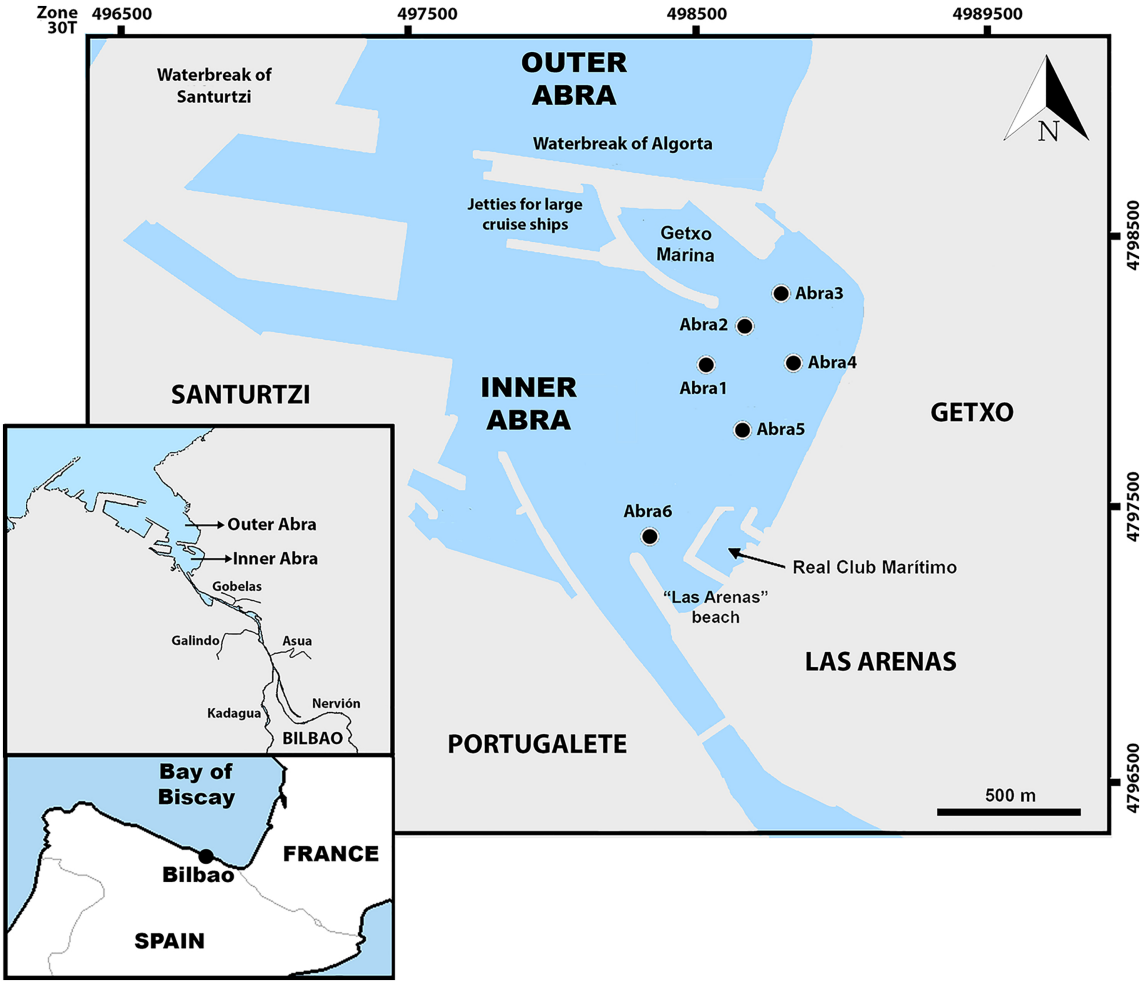
Zone 30T
496500
497500
498500
4989500
4798500
4797500
4796500
OUTER ABRA
Waterbreak of Santurtzi
Waterbreak of Algorta
Jetties for large cruise ships
Getxo Marina
Abra1
Abra2
Abra3
Abra4
Abra5
Abra6
INNER ABRA
SANTURTZI
GETXO
Real Club Marítimo
"Las Arenas" beach
LAS ARENAS
PORTUGALETE
500 m
N
Outer Abra
Inner Abra
Gobelas
Galindo
Asua
Kadagua
Nervión
BILBAO
Bay of Biscay
FRANCE
Bilbao
SPAIN

Figure 1

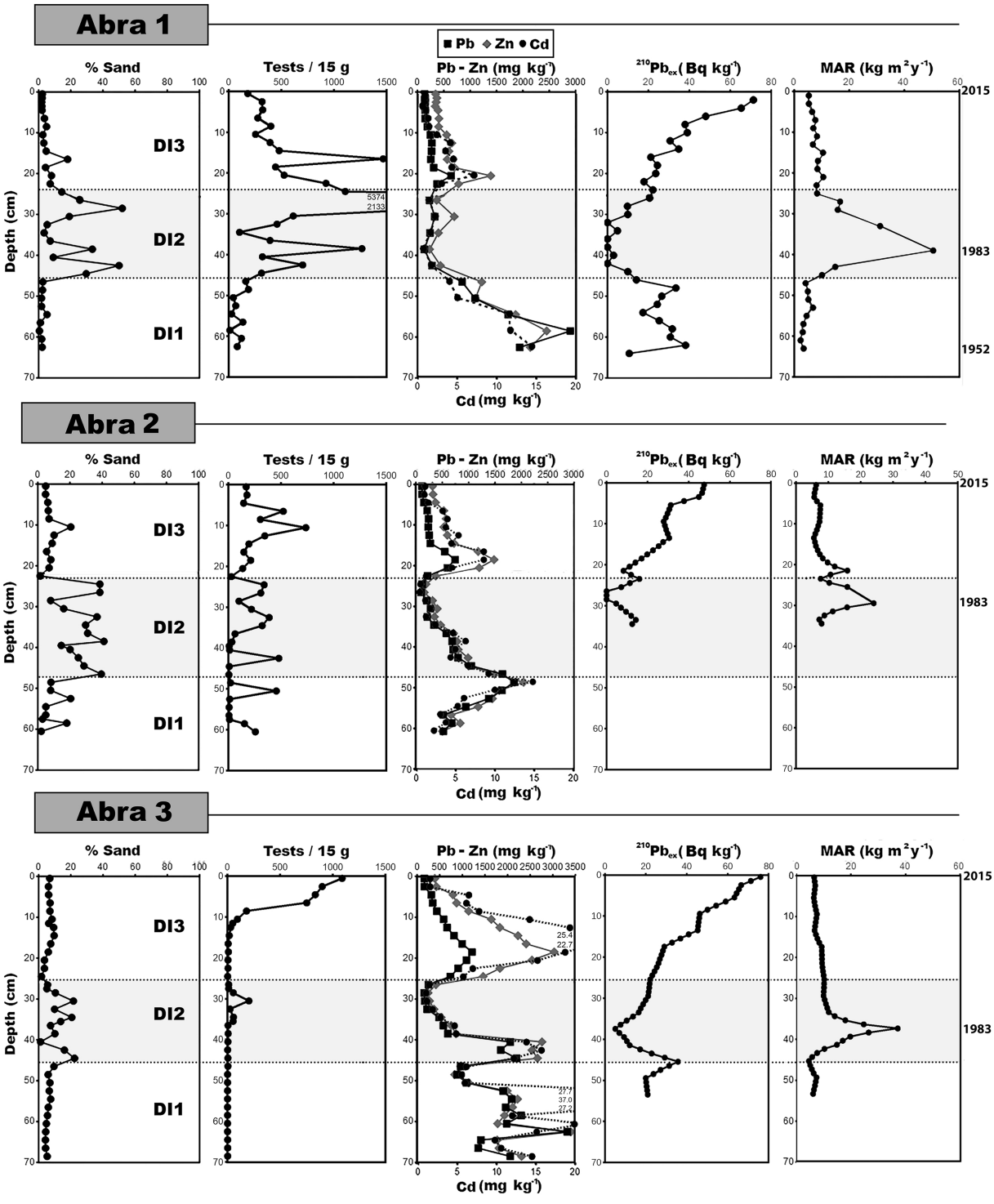
Abra 1
Pb Zn Cd
% Sand
Tests / 15 g
Pb - Zn (mg kg-1)
210Pbex (Bq kg-1)
MAR (kg m2y-1)
Depth (cm)
DI3
DI2
DI1
5374
2133
2015
1983
1952
Cd (mg kg-1)
Abra 2
% Sand
Tests / 15 g
Pb - Zn (mg kg-1)
210Pbex (Bq kg-1)
MAR (kg m2y-1)
Depth (cm)
DI3
DI2
DI1
2015
1983
Cd (mg kg-1)
Abra 3
% Sand
Tests / 15 g
Pb - Zn (mg kg-1)
210Pbex (Bq kg-1)
MAR (kg m2y-1)
Depth (cm)
DI3
DI2
DI1
25.4
22.7
27.7
37.0
27.2
2015
1983
Cd (mg kg-1)

Figure 2

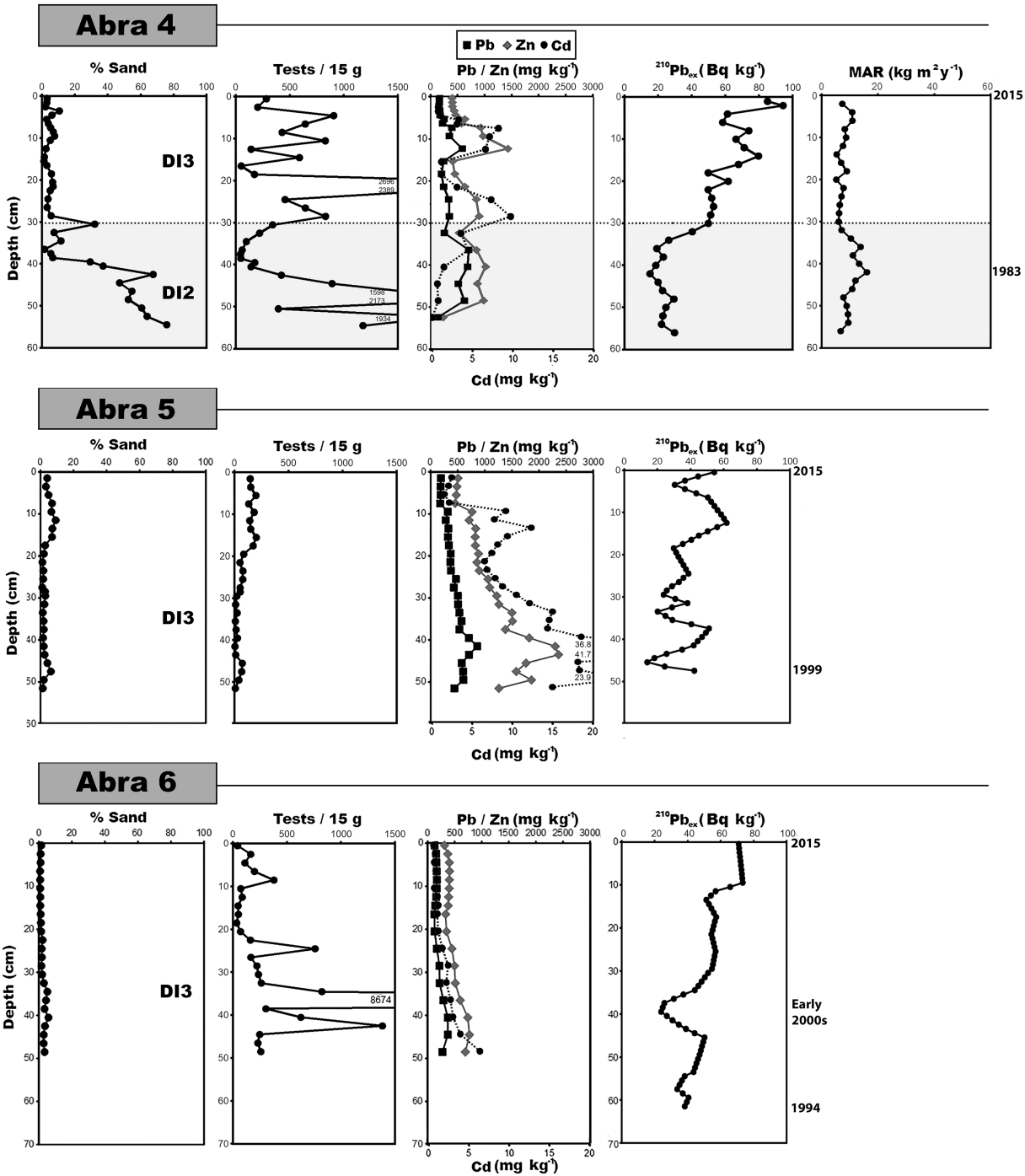
Abra 4
Pb
Zn
Cd
% Sand
Tests / 15 g
Pb / Zn (mg kg-1)
210Pbex (Bq kg-1)
MAR (kg m2y-1)
Depth (cm)
DI3
DI2
2686
2389
1598
2173
1934
Cd (mg kg-1)
2015
1983
Abra 5
% Sand
Tests / 15 g
Pb / Zn (mg kg-1)
210Pbex (Bq kg-1)
Depth (cm)
DI3
36.8
41.7
23.9
Cd (mg kg-1)
2015
1999
Abra 6
% Sand
Tests / 15 g
Pb / Zn (mg kg-1)
210Pbex (Bq kg-1)
Depth (cm)
DI3
8674
Cd (mg kg-1)
2015
Early 2000s
1994

Figure 3

Table 1. Summary of lithological, geochemical and microfaunal data in the Abra bay cores. The single value represents the median and those in parentheses give the range. Metal values in mg kg^{-1}. Total abundances values in number of tests / 15 g of dry sediment.

	Abra 1 (43°20'04.7"N, 3°01'01.0"W)	**Abra 2** (43°20'08.4"N, 3°00'55.8"W)	**Abra 3** (43°20'11.6"N, 3°00'50.6"W)	**Abra 4** (43°20'05.9"N, 3°00'48.3"W)	**Abra 5** (43°19'56.6"N, 3°00'59.8"W)	**Abra 6** (43°19'46.5"N, 3°01'12.8"W)
DI3	Depth interval 24-0 cm Thickness 24 cm Lithology mud Sand 5 (2-18)% Pb 216 (136-640) Zn 481 (339-1390) Cd 2 (1-7) Tests 396 (180-1467) Species 20 (16-24) Marine tests 60 (49-80)% Agglutinated 3 (1-16)% Porcellaneous 5 (1-10)% Hyaline 92 (79-96)% *A. tepida* 34 (13-44)% *R. irregularis* 16 (4-36)% *C. lobatulus* 13 (5-15)% *B. spathulata* 7 (2-17)% *H. germanica* 5 (2-10)% *E. scaber* 4 (1-16)% *B. gibba* 4 (1-13)%	Depth interval 22-0 cm Thickness 22 cm Lithology mud Sand 8 (5-21)% Pb 241 (115-743) Zn 574 (313-1480) Cd 4 (1-9) Tests 195 (135-735) Species 22 (18-28) Marine tests 49 (37-74)% Agglutinated 11 (1-25)% Porcellaneous 4 (0.3-12)% Hyaline 85 (75-94)% *A. tepida* 36 (14-46)% *R. irregularis* 16 (1-46)% *E. scaber* 11 (1-25)% *C. lobatulus* 11 (2-20)% *H. germanica* 6 (3-12)% *B. gibba* 6 (1-12)%	Depth interval 25-0 cm Thickness 25 cm Lithology mud Sand 6 (2-10)% Pb 662 (160-1210) Zn 1640 (391-3030) Cd 8 (2-25) Tests 39 (1-1088) Species 10 (2-20) Marine tests 24 (13-36) Agglutinated 4 (1-11)% Porcellaneous 1 (0-3)% Hyaline 95 (89-97)% *A. tepida* 67 (52-81)% *B. gibba* 6 (4-8)% *C. lobatulus* 6 (3-7)% *E. scaber* 4 (1-11)% *R. irregularis* 2 (1-3)%	Depth interval 30-0 cm Thickness 30 cm Lithology mud Sand 5 (1-11)% Pb 241 (156-583) Zn 573 (397-1420) Cd 3 (1-10) Tests 588 (50-2696) Species 15 (11-21) Marine tests 19 (14-26)% Agglutinated 4 (2-7)% Porcellaneous 1 (0-3)% Hyaline 95 (90-97)% *A. tepida* 73 (53-81)% *B. gibba* 5 (2-10)% *E. scaber* 4 (2-7)% *C. lobatulus* 3 (0-5)% *R. irregularis* 2 (0-8)%	Depth interval >52-0 cm Thickness >52 cm Lithology mud Sand 4 (1-9)% Pb 434 (178-860) Zn 1075 (453-2360) Cd 10 (2-42) Tests 66 (4-201) Species 15 (3-24) Marine tests 31 (8-49)% Agglutinated 4 (0-21)% Porcellaneous 10 (3-61)% Hyaline 86 (40-91)% *A. tepida* 58 (2-79)% *Q. seminula* 7 (2-43)% *E. scaber* 6 (1-21)% *B. gibba* 6 (1-16)% *C. lobatulus* 3 (1-10)% *R. irregularis* 3 (1-8)%	Depth interval >50-0 cm Thickness >50 cm Lithology mud Sand 2 (1-8)% Pb 167 (129-374) Zn 402 (313-772) Cd 1 (0.7-6) Tests 222 (34-8674) Species 26 (14-32) Marine tests 63 (52-80)% Agglutinated 5 (1-12)% Porcellaneous 3 (0.4-10)% Hyaline 92 (84-96)% *A. tepida* 18 (9-32)% *R. irregularis* 13 (3-35)% *B. britannica* 12 (2-26)% *B. spathulata* 8 (3-17)% *B. gibba* 7 (0-17)% *C. lobatulus* 6 (2-12)% *E. scaber* 5 (0.3-12)%
DI2	Depth interval 46-24 cm Thickness 22 cm Lithology sandy mud Sand 23 (3-52)% Pb 240 (130-329) Zn 398 (231-697) Cd 2 (1-2) Tests 613 (102-5374) Species 17 (12-19) Marine tests 69 (58-84)% Agglutinated 2 (0-5)% Porcellaneous 8 (4-11)% Hyaline 90 (84-95)% *R. irregularis* 27 (12-42)% *C. lobatulus* 18 (11-31)% *A. tepida* 18 (9-28)% *H. germanica* 11 (0.3-15)% *Q. seminula* 8 (3-11)% *R. anomala* 6 (5-11)%	Depth interval 48-22 cm Thickness 26 cm Lithology sandy mud Sand 26 (2-41)% Pb 342 (98-1640) Zn 468 (158-1490) Cd 3 (1-9) Tests 81 (4-479) Species 18 (4-25) Marine tests 56 (42-70)% Agglutinated 0 (0-1)% Porcellaneous 6 (4-14)% Hyaline 94 (86-96)% *R. irregularis* 27 (19-35)% *A. tepida* 27 (13-32)% *C. lobatulus* 19 (7-32)% *H. germanica* 10 (7-16)%	Depth interval 45-25 cm Thickness 20 cm Lithology sandy mud Sand 12 (1-22)% Pb 533 (156-2200) Zn 641 (242-2760) Cd 4 (1-16) Tests 11 (1-202) Species 9 (1-18) Marine tests 33 (33-37)% Agglutinated 0 (0-1)% Porcellaneous 1 (1-2)% Hyaline 99 (97-99)% *A. tepida* 32 (30-35)% *H. germanica* 28 (19-30)% *R. irregularis* 18 (14-28)% *C. lobatulus* 8 (4-13)%	Depth interval >56-30 cm Thickness >26 cm Lithology sandy mud Sand 37 (2-76)% Pb 567 (136-701) Zn 853 (234-1010) Cd 1 (0.2-5) Tests 340 (43-2173) Species 20 (15-26) Marine tests 46 (28-65)% Agglutinated 1 (0-17)% Porcellaneous 12 (1-21)% Hyaline 87 (77-93)% *A. tepida* 36 (25-61)% *C. lobatulus* 15 (1-41)% *H. germanica* 6 (4-13)% *R. irregularis* 4 (0-7)%		

DI1	Depth interval >64-46 cm Thickness >18 cm Lithology mud Sand 2 (1-5)% Pb 1720 (848-2900) Zn 1860 (1100-2450) Cd 12 (4-14) Tests 80 (10-187) Species 13 (10-17) Marine tests 82 (69-88)% Agglutinated 0 (0-1)% Porcellaneous 11 (10-40)% Hyaline 89 (61-91)% *R. irregularis* 20 (11-20)% *B. gibba* 17 (8-24)% *C. lobatulus* 15 (11-19)% *Q. seminula* 11 (10-40)% *A. tepida* 8 (5-26)% *B. spathulata* 7 (3-10)% *H. germanica* 5 (4-13)%	Depth interval >61-48 cm Thickness >13 cm Lithology mud Sand 9 (2-20)% Pb 947 (518-1860) Zn 1180 (502-2040) Cd 5 (2-15) Tests 16 (5-455) Species 8 (6-26) Marine tests 41 (38-62)% Agglutinated 2 (0-7)% Porcellaneous 4 (2-11)% Hyaline 92 (89-94)% *A. tepida* 48 (17-50)% *C. lobatulus* 20 (9-21)% *H. germanica* 7 (4-8)% *B. gibba* 5 (4-14)% *R. irregularis* 5 (4-14)%	Depth interval >69-45 cm Thickness >24 cm Lithology mud Sand 6 (4-10)% Pb 1930 (882-3320) Zn 1870 (830-3400) Cd 13 (6-37) Tests 1 (0-4) Species 1 (0-4) Few foraminifera			

Supplementary data to this article can be found online at https://doi.org/10.1016/j.scitotenv.2019.133946.